GeoHealth

RESEARCH ARTICLE
10.1029/2023GH000890

Key Points:

- Geostationary satellite data are able to identify 60% more person-alerts (people × $PM_{2.5}$ alerts) than polar-orbiting satellite data
- Use of geostationary, over polar obiting, satellite data to inform public action on $PM_{2.5}$ alert days could avert an estimated 1,200 deaths
- $PM_{2.5}$ health impacts averted by individual action on geostationary satellite identified alert days are valued at $13 billion ($2019)

Supporting Information:

Supporting Information may be found in the online version of this article.

Correspondence to:

K. O'Dell,
kodell@gwu.edu

Citation:

O'Dell, K., Kondragunta, S., Zhang, H., Goldberg, D. L., Kerr, G. H., Wei, Z., et al. (2024). Public health benefits from improved identification of severe air pollution events with geostationary satellite data. *GeoHealth*, *8*, e2023GH000890. https://doi.org/10.1029/2023GH000890

Received 26 JUN 2023
Accepted 6 OCT 2023

Public Health Benefits From Improved Identification of Severe Air Pollution Events With Geostationary Satellite Data

Katelyn O'Dell[1], Shobha Kondragunta[2], Hai Zhang[3], Daniel L. Goldberg[1], Gaige Hunter Kerr[1], Zigang Wei[3], Barron H. Henderson[4], and Susan C. Anenberg[1]

[1]Milken Institute School of Public Health, George Washington University, Washington, DC, USA, [2]NOAA/NESDIS/Center for Satellite Applications and Research, College Park, MD, USA, [3]I. M. Systems Group, NOAA NCWCP, 5830 University Research Ct, College Park, MD, USA, [4]U.S. EPA Office of Planning and Standards, Durham, NC, USA

Abstract Despite improvements in ambient air quality in the US in recent decades, many people still experience unhealthy levels of pollution. At present, national-level alert-day identification relies predominately on surface monitor networks and forecasters. Satellite-based estimates of surface air quality have rapidly advanced and have the capability to inform exposure-reducing actions to protect public health. At present, we lack a robust framework to quantify public health benefits of these advances in applications of satellite-based atmospheric composition data. Here, we assess possible health benefits of using geostationary satellite data, over polar orbiting satellite data, for identifying particulate air quality alert days (24hr $PM_{2.5} > 35$ μg m^{-3}) in 2020. We find the more extensive spatiotemporal coverage of geostationary satellite data leads to a 60% increase in identification of person-alerts (alert days × population) in 2020 over polar-orbiting satellite data. We apply pre-existing estimates of $PM_{2.5}$ exposure reduction by individual behavior modification and find these additional person-alerts may lead to 1,200 (800–1,500) or 54% more averted $PM_{2.5}$-attributable premature deaths per year, if geostationary, instead of polar orbiting, satellite data alone are used to identify alert days. These health benefits have an associated economic value of 13 (8.8–17) billion dollars ($2019) per year. Our results highlight one of many potential applications of atmospheric composition data from geostationary satellites for improving public health. Identifying these applications has important implications for guiding use of current satellite data and planning future geostationary satellite missions.

Plain Language Summary The systems historically used to monitor air pollution in the US have insufficient spatial coverage to observe all air pollution events. For example, smoke from western wildfires varies rapidly in space and time, making smoke-sourced pollution difficult to track with surface monitors (spatially limited) or global satellites temporally limited to one daily snapshot. Here, we show that new satellites capturing hourly pollution changes over one world region can identify more person-alerts (population × poor air quality alert days) in the US, compared with global satellites, enabling the public to take action to reduce exposure and avoid health consequences. Our results illustrate the health and economic benefits of one pathway to improve the integrated air pollutant monitoring strategy in the US.

1. Introduction

Exposure to fine particulate matter ($PM_{2.5}$) has severe negative impacts on human health. In the United States (US) alone, exposure to ambient $PM_{2.5}$ is estimated to lead to 50,000–200,000 premature deaths (Ford et al., 2018; GBD, 2019; O'Dell et al., 2021; Tessum et al., 2019) and contribute 3%–11% of asthma emergency room visits in the US each year (Anenberg et al., 2018) among other negative health outcomes (U.S. EPA, 2022). Successful regulations of anthropogenic emissions in the US under the Clean Air Act have led to significant reductions in ambient $PM_{2.5}$ concentrations over the past several decades (Malm et al., 2017; McClure & Jaffe, 2018; O'Dell et al., 2019; Ridley et al., 2018). However, in parts of the western US where fires drive interannual variability in summer $PM_{2.5}$ (Jaffe et al., 2008; Spracklen et al., 2007) and contribute up to 75% of summer-mean $PM_{2.5}$ concentrations, particulate air quality has not improved (O'Dell et al., 2019). There, short-term $PM_{2.5}$ pollution events have increased in frequency and intensity in recent years (Childs et al., 2022; McClure & Jaffe, 2018) due to increases in frequency and area burned by large western wildfires (Abatzoglou & Williams, 2016; David et al., 2021; Westerling, 2016).

Satellite-based estimates of surface $PM_{2.5}$ concentrations are continually advancing (van Donkelaar et al., 2021) and can guide exposure-reducing actions to protect public health (Anenberg et al., 2020; Holloway et al., 2021). Surface $PM_{2.5}$ is estimated from satellites by relating satellite observations of columnar aerosol optical depth (AOD) to ground-level $PM_{2.5}$ concentrations with ground-based monitors and/or atmospheric chemistry models (Di et al., 2019; Diao et al., 2019; Hammer et al., 2020; Wang et al., 2018; Zhang & Kondragunta, 2021). These satellite-based data sets have been used to quantify health impacts of $PM_{2.5}$ (e.g., Anenberg et al., 2018; Diao et al., 2019), identify racial and socioeconomic disparities in $PM_{2.5}$ exposure (Castillo et al., 2021; Kerr et al., 2022; Liu et al., 2021), and estimate smoke exposure during wildfire events (e.g., Geng et al., 2018; Rappold et al., 2011). The inclusion of AOD observations on geostationary satellites expands these applications by allowing for observations during all cloud-free daylight hours as opposed to a single daily snapshot from previous polar-orbiting satellites. AOD observations on geostationary satellites began with the Geostationary Operational Environmental Satellites (GOES)-East and GOES-West in 2017 and are expected to be continued into the coming decade(s) by NASA's Tropospheric Emissions: Monitoring Pollution (TEMPO) mission and NOAA's Geostationary Extended Observations (GeoXO) mission (Zoogman et al., 2017).

Quantifying benefits of satellite-based data sets to public health can provide valuable information about the societal improvements from current and future governmental investments in Earth observing satellites with atmospheric composition instrumentation. These potential benefits include near real time identification of pollution events (e.g., Huff & Kondragunta, 2017), assessment of sub-daily patterns in emissions sources which could inform more effective emissions-reduction strategies, and more accurate estimates of surface $PM_{2.5}$ (e.g., Zhang et al., 2022). Currently, GOES provides observations of AOD over the contiguous US every 5 min during daylight hours (Kondragunta et al., 2020; Schmit et al., 2005; Zhang & Kondragunta, 2021). GOES-based AOD observations have already been used to help capture short-term pollution events in near real time or "nowcasting" (Huff et al., 2021; Vu et al., 2022; Zhang et al., 2022). This application of current and future geostationary atmospheric composition data is especially important for wildfire-driven $PM_{2.5}$ pollution events, which can often be difficult to capture in monitoring networks due to wildfire smoke's high temporal and spatial variability (Huff & Kondragunta, 2017; O'Neill & Raffuse, 2021). At present, we lack a robust framework to quantify potential health benefits of this application of geostationary atmospheric composition data.

In this work, we develop a methodology to quantify the potential health benefits of $PM_{2.5}$ nowcasting satellite-based atmospheric composition data. We use estimates of 24hr mean surface $PM_{2.5}$ derived from both polar-orbiting satellites (one observation per day on cloud-free days) and geostationary satellites (observations during all cloud-free daylight hours) previously estimated by Zhang et al. (2022). Within these data sets, we flag days where the 24hr mean $PM_{2.5}$ exceeds 35.45 μg m^{-3}, the threshold for "code orange" particulate air quality alert days and approximating the current 24hr National Ambient Air Quality Standard (NAAQS) of 35 μg m^{-3} for $PM_{2.5}$. Previous works have found that alerted populations take individual actions to reduce exposure to poor air quality (Burke et al., 2022; Rappold et al., 2017; U.S. EPA, 2021) and this can benefit public health (Chen et al., 2018). We apply previously calculated multi-study estimates of personal $PM_{2.5}$ exposure reduction on poor air quality days and conduct a health impact assessment to estimate averted $PM_{2.5}$-attributable mortality and morbidity. For comparison, we also apply this framework to estimate alert days identified by monitor based $PM_{2.5}$ nowcasting. The framework developed here to quantify health benefits of reductions in $PM_{2.5}$ exposure from this alerted behavior modification pathway can be applied to quantify benefits of future improvements in air quality nowcasting and geostationary satellite-based observations of atmospheric composition.

2. Materials and Methods

2.1. $PM_{2.5}$ Data Sets

We use four data sets of daily, surface $PM_{2.5}$ concentrations in 2020 to investigate the possible benefits of different data sources for use in air quality nowcasting. While 2020 was an anomalously active fire year, fire years like 2020 are projected to become more likely in the future (Abatzoglou et al., 2021; Xie et al., 2022), when new geostationary satellites that are presently in the planning phase and could be informed by our analysis (like GeoXO) will be operational. The three satellite-based data sets of surface $PM_{2.5}$ we use are described in detail by Zhang et al. (2022). We will provide a brief description here and refer readers to Zhang et al. (2022) for additional details. The three data sets rely on three different sources of AOD, described in the following paragraph, which are used to estimate 24hr mean surface $PM_{2.5}$ concentrations by a geographically weighted regression algorithm.

The algorithm assumes linear relationships between $PM_{2.5}$ and AOD varying with space and time. It derives the relationships at each time step from the surface $PM_{2.5}$ measurements and AOD matchup data set. In this work, we regrid all surface $PM_{2.5}$ estimates from by Zhang et al. (2022) to a 0.01° × 0.01° grid (approximately 1 km × 1 km).

AOD observations are obtained from the ABI sensor onboard GOES-16 and GOES-17 and the VIIRS sensors onboard the NOAA-20 and Suomi National Polar-orbiting Partnership (SNPP) satellites. The ABI sensor has 16 spectral bands and a resolution of 2 km at nadir. It retrieves AOD at 550 nm at a temporal resolution of approximately 5 min during all cloud-free daylight hours (Schmit et al., 2005, 2018). The VIIRS sensor onboard SNPP and NOAA-20 retrieves AOD at 550 nm at approximately 1:30 pm local time if there is no interference from clouds (Liu et al., 2014; Zhang et al., 2016). The sensor has 22 spectral bands and a 0.75 km resolution at nadir. We use bias corrected ABI AOD with high and medium qualities (Zhang et al., 2020) and VIIRS high quality AOD. To represent geostationary satellite-based nowcasting, we use 24hr mean surface $PM_{2.5}$ concentrations estimated using hourly ABI AOD from all daylight hours. We refer to this data set as ABI-Daytime. To represent polar-orbiting satellite-based nowcasting, we use 24hr mean surface $PM_{2.5}$ concentrations estimated with VIIRS AOD observed at 1:30 p.m. local time. The VIIRS-based data set represents a true polar-orbiting case but uses a different retrieval algorithm compared with ABI.

Because there are differences between the VIIRS and ABI sensors, such as different processing algorithms and spatial resolutions, we also created a third data set to isolate the impacts of the difference in temporal coverage between geostationary and polar-orbiting satellites. To create the ABI-1pm data set, we use the ABI-Daytime estimated surface $PM_{2.5}$ values, but only for grid cells where the ABI AOD has a retrieval at 1 p.m. local time. This data set mimics the temporal and spatial completeness of surface $PM_{2.5}$ estimates based on a polar-orbiting satellite while quantitatively agreeing with surface $PM_{2.5}$ estimated in the ABI-Daytime data set. The ABI-1pm data set thus isolates the impacts of the difference in temporal coverage between geostationary and polar-orbiting satellites by using the same retrieval algorithm and AOD to $PM_{2.5}$ conversion for both. We note that our ABI-1pm data set, and subsequent comparison to ABI-Daytime, does not include the improved accuracy of surface $PM_{2.5}$ estimates with the additional data available in ABI-Daytime. This benefit of geostationary satellite data is described by Zhang et al. (2022) by analyzing surface-monitor $PM_{2.5}$. They reported correlations between $PM_{2.5}$ at 1 p.m. and daily $PM_{2.5}$ are generally above 0.6 across the continental US, while that for daytime $PM_{2.5}$ and daily $PM_{2.5}$ are above 0.8 (Zhang et al., 2022, Figure 6). In addition, the ABI-Daytime data set (when compared to surface monitors) has an estimated coefficient of determination ranging from 0.26 to 0.86 and a mean bias from −1 to 1 μg m^{-3}, varying by US state (Zhang et al., 2022, Figure 3).

To represent monitor-only based nowcasting (the state of the art at the national level), we use 24hr mean $PM_{2.5}$ observations from ground-level monitors in the EPA's AirNow network (US EPA, 2023). With this data set, which we refer to as AirNow-RA, we attempt to replicate the spatial coverage of the NowCast value AirNow reports to a user based on their location. We assign the concentrations reported at monitors to the surrounding zip code tabulation areas (ZCTAs) by calculating a single concentration to represent an entire "reporting area." Reporting areas are a feature of AirNow that specify the region for which a forecast is made and all monitors within that area (e.g., a city) are considered representative. The NowCast is typically reported hourly, where the maximum hourly value among all the monitors located in a particular reporting area is applied to the respective reporting area each hour. Here, we take the max of the 24hr mean $PM_{2.5}$ observed by all monitors in each reporting area for a daily NowCast value to align with the temporal resolution of the satellite-based surface $PM_{2.5}$ estimates.

For each of the data sets, ABI-Daytime, ABI-1pm, VIIRS, and AirNow-RA we determine the number of estimated air quality alert days and the total population in alerted grid cells/ZCTAs. For the gridded satellite-based data sets, we use gridded estimates of population in 2020 from the NASA Socioeconomic Data and Applications Center (SEDAC) Gridded Population of the World, version 4.11 (GPW, v4.11) regridded to the 0.01° × 0.01° $PM_{2.5}$ grid from an original resolution of 2.5 × 2.5 arcminutes (NASA SEDAC, 2018). With the reporting-area level AirNow-RA data set, we use 2020 population estimates by ZCTA from the 2020 census accessed through the National Historical Geographic Information System (Manson et al., 2022). We note these data sets and the subsequent identification of alerted populations used in this work do not reflect how these data sources may be used in practice to inform the public of air quality alert days. Here, we use these data sets to show the availability of $PM_{2.5}$ concentration data from different data sources for use by air quality forecasters and investigate how this additional information may benefit public health.

2.2. $PM_{2.5}$ Reduction by Behavior Modification

We quantify the health benefits of air quality alerts by assuming alerted communities modify their behavior to reduce their personal $PM_{2.5}$ exposure. Research studies on behavior modification decisions and effectiveness of different actions during smoke events were summarized in the Comparative Assessment of the Impacts of Prescribed Fire Versus Wildfire (CAIF) report by the US EPA (U.S. EPA, 2021, Table 6-1). The CAIF report provides effective exposure reduction values that account for both the fraction of people who take specific exposure-reducing actions and the estimated mean $PM_{2.5}$ exposure reduction from the actions. The CAIF report provides multiple estimated reductions in $PM_{2.5}$, with mean values ranging from 15% to 30%, depending on the action. We chose the 30% reduction value estimated for remaining indoors because it is associated with the highest likelihood of taking action (60%) with an associated $PM_{2.5}$ reduction effectiveness estimate (50%) in the CAIF report. The resulting average overall exposure reduction for the behavior modification action of remaining indoors is 30% (0.60 taking action × 0.50 effectiveness) and likely represents an upper bound on population exposure reduction from individual-level action.

There is likely a high degree of uncertainty and possible geographic variability in the reduction in population $PM_{2.5}$ exposure on alert days. We test the sensitivity of our results to this value by conducting our analysis using the reported standard deviation of the multi-study mean likelihood of remaining indoors and effectiveness of remaining indoors for exposure reduction provided in the EPA CAIF report (U.S. EPA, 2021, Table 6-1). This gives a lower bound of 15% and upper bound of 50% reduction in $PM_{2.5}$. We note these values are specific to smoke-impacted pollution events, which may have a higher degree of awareness than non-smoke impacted pollution events. For example, a recent survey of residents in the Washington, DC metro area (far from large western wildfires) estimated a 23% likelihood of remaining indoors (Clean Air Partners, 2018). Assuming the same action effectiveness (50%), this results in an overall exposure reduction value of 12%, close to the lower bound exposure reduction value of 15% we use here. However, given 2020 was an active fire year with significant impacts on air pollution in populated areas, it is likely a majority of the alert days in our data set are impacted by smoke events. The details of our sensitivity analysis to the percent exposure reduction value are provided in the supplement.

We apply these reductions in $PM_{2.5}$ exposure from air quality alerts and subsequent behavior modification to the two ABI-based nowcasting data sets. We don't apply the exposure reduction and health impact assessment calculations to the VIIRS-based and monitor-based data sets because there are quantitative differences in the underlying $PM_{2.5}$ estimates which will also impact the health impact assessment results and thus make the impacts of additional spatial coverage and/or higher spatial resolution unclear. Thus, for the two ABI-based data sets only, we reduce $PM_{2.5}$ by 30% in grid cells where the estimated 24hr average $PM_{2.5}$ is >35.45 μg m^{-3} (air quality alert days). On non-alert days, $PM_{2.5}$ exposure is taken as the estimated ambient concentration.

2.3. Health Impact Assessment

We use the following health impact function from Anenberg et al. (2010, 2014) to estimate the health benefits of reduced $PM_{2.5}$ exposure,

$$E = P \times \mathrm{BR} \times (1 - \exp(-\beta \times \Delta \mathrm{PM}_{2.5})), \quad (1)$$

where E is the attributable health events, P is the population, BR is the baseline event rate, $\Delta PM_{2.5}$ is the estimated $PM_{2.5}$ exposure minus the theoretical concentration at which minimal excess risk occurs, and β is defined as,

$$\beta = \ln(\mathrm{RR})/X, \quad (2)$$

where RR is the relative excess risk per an X increase in $PM_{2.5}$ concentration. This equation assumes a linear relationship between $PM_{2.5}$ concentrations and the log of relative risk and has been previously applied in several studies quantifying public health impacts of short-term and long-term exposure to $PM_{2.5}$ (Anenberg et al., 2010, 2018; Ford et al., 2018; O'Dell et al., 2021).

Equations 1 and 2 are used to estimate both $PM_{2.5}$-attributable premature mortality and asthma emergency room visits. As higher resolution rates are not available, we use a national baseline rate for asthma emergency room visits of 50.2 visits per 10,000 people, obtained from Centers for Disease Control reports based on data from the Healthcare Cost Utilization Project for the year 2018 (AHRQ, 2006; Healthcare Use Data | CDC, 2023). We use a RR of asthma emergency room visits of 1.03 (95% CI: 1.01, 1.05) from Orellano et al. (2017) with a threshold

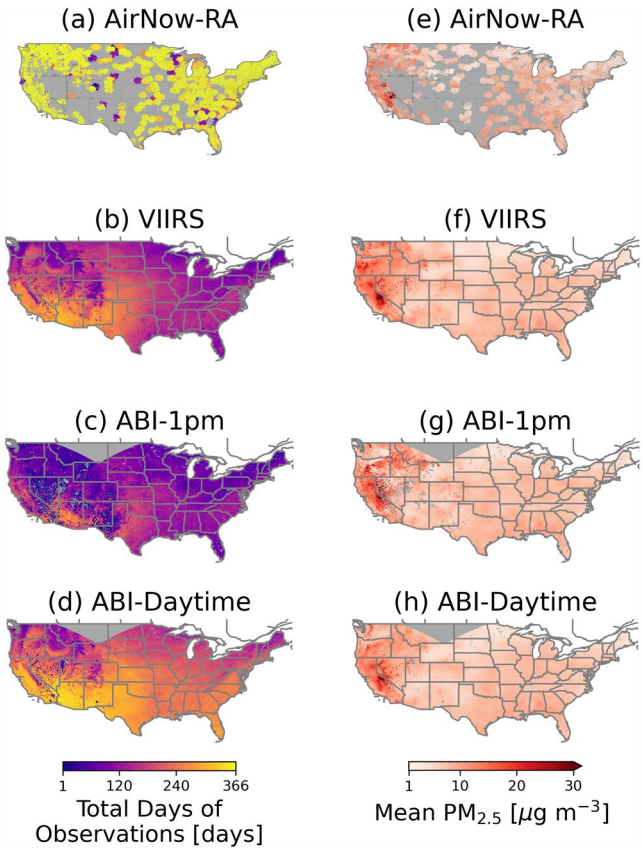

Figure 1. Total days of observations (panels b–d) and annual mean $PM_{2.5}$ (panels f–h) in 2020 for three satellite based $PM_{2.5}$ data sets. Panels (a, e) show total observations and annual mean $PM_{2.5}$ for the AirNow reporting areas (RA) by ZipCode Tabulation Area (ZCTA), respectively. Gray areas indicate locations without observations.

concentration of 0 μg m^{-3}. Total population estimates for the year 2020 are obtained from the NASA SEDAC Gridded Population of the World v4.11 at 2.5 arcminute resolution (NASA SEDAC, 2018) and regridded to the same 0.01° × 0.01° grid as the $PM_{2.5}$ concentration estimates. We apply Equation 1 with these inputs and 24hr mean $PM_{2.5}$ to estimate the $PM_{2.5}$-attributable asthma emergency room visits for each grid cell on each day. We sum the $PM_{2.5}$-attributable asthma emergency room visits across all days in 2020 and all grid cells to estimate the national annual total of $PM_{2.5}$-attributable asthma emergency room visits.

To estimate attributable premature mortality, we use a RR for long-term exposure to $PM_{2.5}$ of 1.06 (95% CI: 1.04, 1.08) from Turner et al. (2016) with a threshold concentration of 2.8 μg m^{-3}, the minimum $PM_{2.5}$ exposure estimated in Turner et al. (2016). We obtain county-level all-cause baseline mortality rates for all ages from the CDC WONDER database averaged over the years 2015–2019 and grid these values to the 0.01° × 0.01° $PM_{2.5}$ grid (CDC, 2021). Here, we again use the regridded total population estimates from the NASA SEDAC Gridded Population of the World v4.11 described above. Annual mean $PM_{2.5}$ is calculated for each data set for use in the mortality estimates to approximate the long-term $PM_{2.5}$ exposures used to develop the concentration response function. We use the annual mean $PM_{2.5}$ with the inputs described above in Equations 1 and 2 to calculate $PM_{2.5}$-attributable mortality at each grid cell. This process is repeated for the baseline ABI-Daytime based $PM_{2.5}$ exposure and the two reduced $PM_{2.5}$ exposure data sets using ABI-Daytime and ABI-1pm identified alert days. The difference between the baseline data set and the reduced data sets based on ABI-Daytime and ABI-1pm derived alerts gives the asthma emergency room visits and mortality that could theoretically be averted with geostationary and polar-orbiting satellite informed nowcasting, respectively.

Finally, we perform an economic valuation of the averted asthma emergency room visits and mortality from nowcasting-informed behavior modification. We follow guidance from the US EPA on economic valuation of health events and mortality (U.S. EPA, 2010). Asthma emergency room visits are valued at $430 ($2010) using a cost-of-care approach (U.S. EPA, 2021). We update this value to $500 ($2019) using the US Bureau of Labor Statistics Consumer Price Index inflation calculator. For an economic valuation of averted premature mortality, we use a value of statistical life of $10.9 million ($2019) calculated using a willingness to pay approach (US DOT, 2023).

3. Results

3.1. Spatial Coverage and Resolution of $PM_{2.5}$ Data Sets for Nowcasting

The AirNow data set of surface $PM_{2.5}$ monitors, as applied by the Environmental Protection Agency (EPA) to Reporting Areas for NowCasting (AirNow-RA), has the greatest temporal completeness where values are reported, but there are large spatial gaps with no data (Figure 1a). On average, the AirNow-RA data set covers ZCTAs spanning 3.8 million km^2 each day, or 54% of the total contiguous US ZCTA area. This data set has the lowest spatial resolution of the four data sets (Figure 1a) because a single maximum 24hr mean $PM_{2.5}$ value is applied across the entire reporting area. We note multiple monitors are available in many of the reporting areas over which air quality nowcast alerts are issued and higher resolution $PM_{2.5}$ concentration estimates could be created with the AirNow monitor data such as with interpolation. However, in the AirNow-RA data set we have attempted to replicate the spatial coverage and resolution of the EPA NowCast, which reports a single value within each reporting area to users.

The two data sets representing polar-orbiting products, VIIRS and ABI-1pm, generally have broader spatial coverage, but a lower annual temporal completeness compared to the AirNow-RA data set (Figures 1a–1c). On

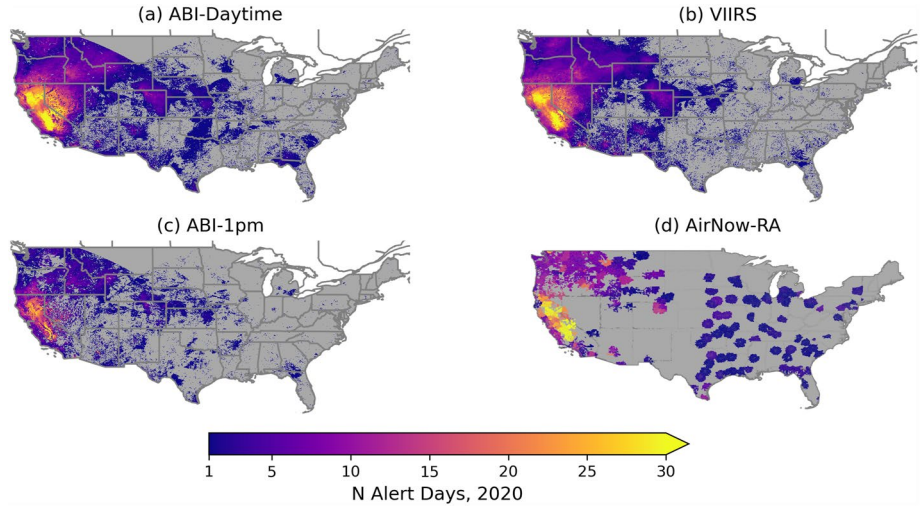

Figure 2. Number of days in 2020 flagged as air quality alert days (24-hr mean $PM_{2.5}$ > 35.45 μg m^{-3}) in each of the four data sets. Gray areas indicate locations with zero identified alert days or no available observations.

average, the VIIRS and ABI-1pm data sets cover 3.5 and 2.1 million km^2 each day or 45% and 27% of the contiguous US grid area in 2020, respectively. The ABI-1pm data set, in most locations, has fewer observations than VIIRS due to differences in retrieval algorithms, spatial resolution of AOD (originally 0.75 km for VIIRS and 2 km for ABI at nadir) and subsequent impacts on cloud masking capabilities, and the lack of ABI retrievals over bright surfaces (e.g., the desert southwest US).

ABI-Daytime, which represents air quality observations from a geostationary satellite, generally provides the most annually complete temporal coverage of 24hr mean $PM_{2.5}$ among the satellite-based data sets (Figure 1d). Like VIIRS and ABI-1pm, the ABI-Daytime data set also has a higher spatial resolution and broader spatial coverage than the AirNow-RA estimates. We note both ABI-Daytime and ABI-1pm have a swath of missing data over eastern Montana and North Dakota. In this location, the two satellites which host an ABI sensor, GEOS-East and GEOS-West, have large view zenith angles for which retrievals are assigned a lower quality. To maintain higher quality data, we remove these retrievals from our analysis. Overall, the ABI-Daytime data set has the highest average daily spatial coverage of all data sets (including AirNow-RA) with a mean of 4.6 million km^2 (59% of contiguous US grid area) covered each day. The 2020 annual mean $PM_{2.5}$ estimated with the ABI-Daytime data set is 8.1 μg m^{-3} (Figure 1h). This is slightly lower than the annual mean $PM_{2.5}$ estimated with AirNow-RA, ABI-1pm, and VIIRS of 8.4 μg m^{-3} (Figures 1e–1g). Although the ABI-1pm data set used here has the same daily $PM_{2.5}$ values as the ABI-Daytime data set by design, the inclusion of different days in the annual average (only days where there is a retrieval at 1 p.m. local time) leads to differences in the estimated annual mean $PM_{2.5}$.

3.2. Alert Days Identified Across the Four Data Sets

ABI-Daytime and VIIRS estimate a similar number of national population-weighted average alert days but follow different spatial patterns. VIIRS estimates a national population-weighted average of 2.4 alert days in the US in 2020 compared to 2.7 annual population-weighted mean alert days in ABI-Daytime. The spatial differences between particulate air quality alert days identified in ABI-Daytime and VIIRS are driven both by differences in spatial and temporal completeness as well as quantitative differences in estimated $PM_{2.5}$ concentrations each day (Figure 2). As shown in Figures 2a and 2b (and the difference plot in Figure S1a in Supporting Information S1), VIIRS estimates more alert days than ABI-Daytime in the northwestern states and desert southwest. In addition to quantitative differences in estimated surface $PM_{2.5}$ concentrations, this could be due to the higher native pixel resolution (750 m vs. 2 km) and stronger capability to retrieve over bright surfaces with the VIIRS sensor discussed previously. We find, nationally, the overall performance of VIIRS and ABI-Daytime at identifying alert days is fairly similar; both data sets have a ~70% probability of correctly identifying an alert day in 2020 (Table S1 in Supporting Information S1). The AirNow-RA alerts (Figure 2d) generally follow a similar spatial pattern to these satellite-based alert days and have a higher number of annual population-weighted mean alerts (3.3), but AirNow-RA has much wider alert areas due to assignment of monitors to broad reporting areas.

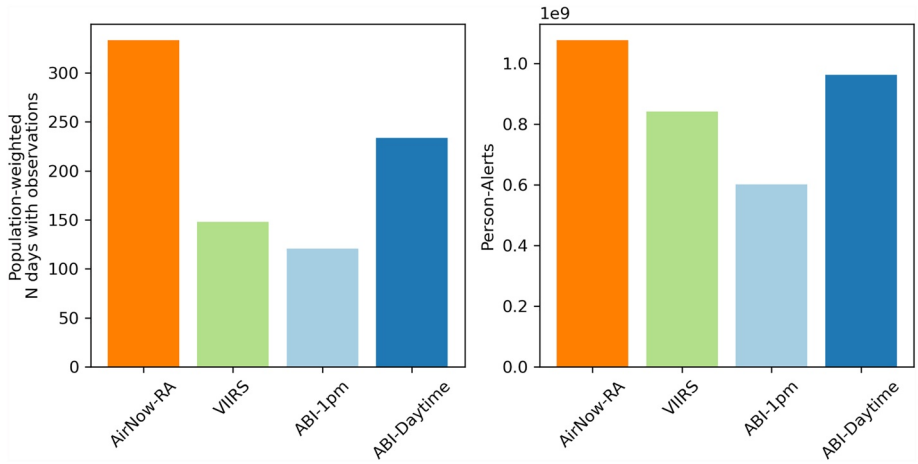

Figure 3. Population-weighted number of days with estimates of 24hr mean $PM_{2.5}$ for each data set (left) and total contiguous US person-alerts (24-hr mean $PM_{2.5} > 35.45$ μg m^{-3}) in each dataset (right) in 2020.

Comparing ABI-1pm and ABI-Daytime removes the influence of algorithm and quantitative differences in estimated $PM_{2.5}$ concentrations. Differences in alert days between these two data sets are thus driven entirely by differences in temporal and spatial completeness each day. As shown in Figure 1, ABI-Daytime has more complete spatial coverage than ABI-1pm due to additional daytime observations. In Figures 2a and 2d (and the difference plot in Figure S1b in Supporting Information S1), we show this also leads to a larger number of observed alert days. On average, ABI-1pm estimates 1.7 annual population-weighted mean alert days in 2020 across the US, much lower than that estimated by ABI-Daytime (2.7 alert days). In total, 57% of the grid cell level alert days identified in the ABI-Daytime data set in 2020 were missed in the ABI-1pm data set due to cloud coverage at the single overpass time. The single overpass was likely missing observations due to partial cloud cover that is not present all day, which allows the ABI-Daytime to report more days.

In all data sets, particulate air quality alert days are predominantly concentrated in California but are not exclusive to California (Figure 2). The spatial distribution of particulate air quality alert days will likely be different for different years as there is high interannual variability in wildfire driven-$PM_{2.5}$ (Jaffe et al., 2008; Spracklen et al., 2007), which is likely contributing to many of the alert days (Childs et al., 2022; David et al., 2021).

We relate the spatial distribution of the number of $PM_{2.5}$ observations (Figure 1) to population and calculate total person-alerts (product of population and number of alerts for each grid cell or ZCTA) for each data set in Figure 3. We find that in 2020 the AirNow-RA data set has the largest population coverage with valid 24hr $PM_{2.5}$ estimates for an average of 333 days (national, population-weighted mean) and the largest number of person-alerts of 1.1 billion. However, as noted previously, the spatial resolution of these alerts is much lower than the satellite-based data sets as a single monitor value is assigned across the reporting areas (Figure 2). When we apply the monitors only to the population in the census tract in which they are located (a closer spatial comparison to the satellite data sets, but not representative of how the monitors are designed to be used in practice) we find only 5 population-weighted number of observation-days and 23 million person alerts in 2020. Of the satellite-based data sets, ABI-Daytime has the highest population coverage with a population-weighted mean 234 days per year, followed by 148 days for VIIRS and 121 days for ABI-1pm. The ABI-Daytime data set also contains the largest number of person-alerts of the satellite-based data sets in 2020 at 960 million person-alerts (Figure 3b). The ABI-Daytime data set identifies more person-alerts than the ABI-1pm (+60%) and VIIRS (+14%) data sets. Although we use these data sets to identify air quality alert days and alerted populations, we again note that they do not directly represent the air quality alerts people currently receive from AirNow or would receive if satellite data were incorporated into nowcasting. Here, we use these data sets as an initial step to investigate if incorporating satellite data, in particular geostationary satellite data, in nowcasting could benefit public health.

3.3. Estimated Reductions in $PM_{2.5}$ Exposure

Due to the higher spatial coverage available through geostationary satellite-based $PM_{2.5}$ estimates and subsequent higher number of alert days identified, the ABI-Daytime based alerts and assumed exposure-reducing behavior

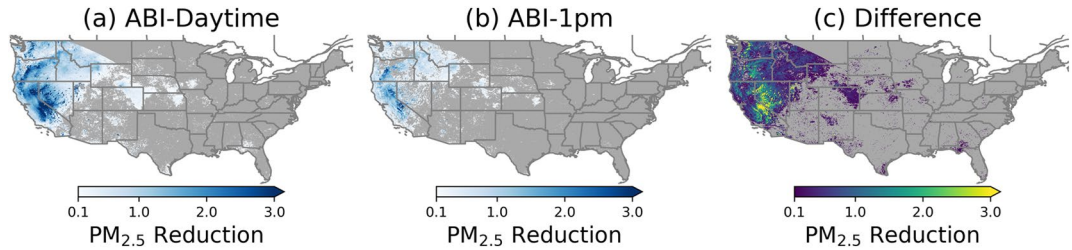

Figure 4. Reduction in annual mean $PM_{2.5}$ exposure due to behavior modification from poor air quality alerts (24-hr mean $PM_{2.5}$ > 35.45 μg m^{-3}) based on data from ABI-Daytime (panel a) and ABI-1pm (panel b). Panel c shows the difference in the estimated annual mean $PM_{2.5}$ exposure reduction estimated using ABI-Daytime and ABI-1pm (panels a, b). Gray areas indicate locations with no reduction in annual mean $PM_{2.5}$ and white areas are locations where no reliable ABI data is available.

modification lead to a larger estimated reduction in annual mean $PM_{2.5}$ exposure than the ABI-1pm based alerts (Figure 4). We only estimate exposure reduction in the two ABI-based data sets, which quantitatively agree on estimates of daily $PM_{2.5}$ by design, unlike the AirNow-RA and VIIRS data sets. We assume a 30% reduction in $PM_{2.5}$ exposure associated with behavior modification on alert days based on a multi-study mean of responses to air pollution during smoke events. We find a national average reduction in estimated $PM_{2.5}$ exposure from individual behavior modification on ABI-Daytime based alert days of 0.2 μg m^{-3}, with the largest reductions occurring in central California. The reduction in $PM_{2.5}$ exposure estimated from ABI-1pm based alerts follows a similar spatial pattern, but the absolute exposure reductions are smaller with a national mean reduction of 0.1 μg m^{-3}. We estimate national, population-weighted $PM_{2.5}$ exposure is reduced by 2% using the ABI-Daytime data set and by 1% using the ABI-1pm data set. For the California population, the change in population-weighted $PM_{2.5}$ exposure is over 7% for ABI-Daytime based alerts and 4% for ABI-1pm based alerts. Like the total estimated reductions in annual mean $PM_{2.5}$ exposure, the additional reductions in the geostationary case are not evenly distributed across the country (Figure 4c). Overall, we find a national average of 0.1 μg m^{-3} additional reduction in mean $PM_{2.5}$ exposure using ABI-Daytime based alerts compared to ABI-1pm based alerts. In Figures S2 and S3 in Supporting Information S1 we show these estimated reductions in annual-mean $PM_{2.5}$ exposure when we assume a 15% and 50% exposure reduction on alert days, respectively, representing the estimated standard deviation of the 30% exposure reduction estimate (U.S. EPA, 2021). We discuss the implications of this uncertainty on our results in the discussion section.

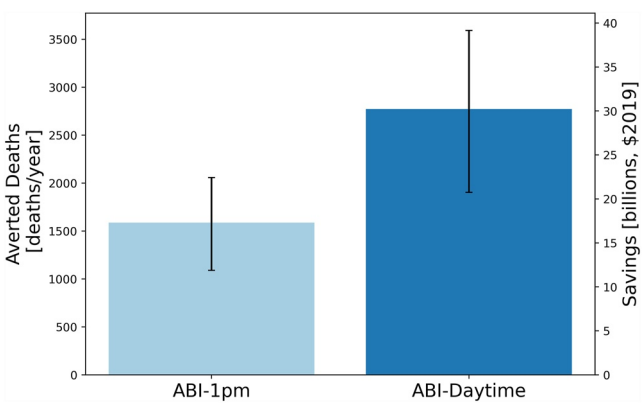

Figure 5. All-cause $PM_{2.5}$-attributable premature deaths averted (left *y*-axis) and associated economic value (right *y*-axis) with behavior modification from poor air quality alerts (24-hr mean $PM_{2.5}$ > 35.45 μg m^{-3}) identified using $PM_{2.5}$ estimates based on ABI-1pm and ABI-Daytime. Error bars indicate uncertainty in averted deaths as defined by the 95% confidence interval in the relative risk used in the health impact function.

3.4. Health and Economic Benefits

We use a health impact assessment to estimate an additional 1,200 (95% CI: 800–1,500) $PM_{2.5}$-attributable premature deaths per year (1% of all $PM_{2.5}$-attributable deaths) could be averted due to the additional exposure reduction with air quality alerts from geostationary satellite (ABI-Daytime) based $PM_{2.5}$ concentration estimates over polar-orbiting satellite (ABI-1pm) based $PM_{2.5}$ concentration estimates (Figure 5). First, before applying reductions due to assumed behavior modification, we estimate a total of 96,000 (95% CI: 65,000–126,000) deaths attributable to $PM_{2.5}$ in the US per year based on total 2020 annual mean concentrations. We subsequently estimate that using geostationary (ABI-Daytime) based $PM_{2.5}$ data for air quality alerts could avert 2,800 (95% CI: 1,900–3,600) $PM_{2.5}$-attributable premature deaths annually, while 1,600 (95% CI: 1,100–2,100) $PM_{2.5}$-attributable deaths could be averted with polar orbiting satellite (ABI-1pm) based $PM_{2.5}$ estimates compared to a scenario with no air quality alerts/behavior modification (Figure 5). In the Supporting Information S1, we also calculate averted deaths from short-term $PM_{2.5}$ exposure (Table S2 in Supporting Information S1) using Equation 1 with a relative risk estimate from Dai et al. (2014). We estimate an additional 210 (95% CI: 160–250) additional averted premature deaths from avoided short-term $PM_{2.5}$ exposure nationwide in 2020 using geostationary over polar-orbiting satellite based alerts.

Using an economic value of statistical life of 10.9 million dollars ($2019; US DOT, 2023) the 2,800 ABI-Daytime averted deaths and 1,600 ABI-1pm averted deaths are valued at 30 billion and 17 billion dollars per year, respectively. The additional 1,200 (95% CI: 800–1,500) $PM_{2.5}$-attributable premature deaths averted with geostationary satellite-based alerts are economically valued at 13 (95% CI: 8.8–17) billion dollars per year ($2019). These estimated averted premature deaths are also sensitive to our assumed 30% exposure reduction via behavior modification on alert days. Assuming a 15% or 50% exposure reduction instead results in an uncertainty range of 590–2,000 deaths (Table S3 in Supporting Information S1), of similar magnitude to the reported 95% CI bound on the health impact function. While the absolute number of estimated averted deaths is sensitive to this assumption, we note the percent difference in alert/behavior modification averted deaths between ABI-1pm and ABI-Daytime based alerts of 54%, is robust.

We similarly estimate 240 (95% CI: 90–340) $PM_{2.5}$-attributable asthma emergency room visits per year (1% of all $PM_{2.5}$-attributable asthma emergency room visits) could be averted with geostationary satellite based air quality alerts over polar-orbiting satellite based alerts. A total of 29,000 (95% CI: 10,000–48,000) asthma emergency room visits in 2020 were attributable to $PM_{2.5}$, based on the total $PM_{2.5}$ concentration estimates in the ABI-Daytime data set. We find 610 (95% CI: 240–890) and 370 (95% CI: 140–550) of these $PM_{2.5}$-attributable emergency room visits could be avoided with geostationary satellite and polar orbiting satellite based alerts, respectively. The additional 240 (95% CI: 90–340) $PM_{2.5}$-attributable asthma emergency room visits averted with geostationary satellite-based alerts are associated with an economic benefit of 120,000 (95% CI: 45,000–170,000) dollars per year ($2019).

We find a majority of the $PM_{2.5}$ alert days identified in each data set and subsequent averted deaths and asthma emergency room visits occur in the western US in 2020. Specifically, 64% of the additional averted $PM_{2.5}$-attributable asthma emergency room visits and 58% of the additional averted $PM_{2.5}$-attributable premature deaths occur in California alone in 2020. The spatial distribution of these benefits will likely vary for different years due to interannual variability in emissions (e.g., wildfire occurrence). However, we expect these benefits to predominantly occur in the western US in most years, where there are now more frequent short-term $PM_{2.5}$ pollution events due to increases in the frequency and intensity of large western wildfires (Childs et al., 2022).

4. Conclusions

In this work, we show that atmospheric composition information from geostationary satellites could lead to a greater reduction in personal exposure to air pollution and subsequently greater public health benefits compared to similar information from polar-orbiting satellites. Specifically, we find estimates of surface $PM_{2.5}$ based on AOD observations from a geostationary satellite are able to identify more particulate air quality alert days (24hr $PM_{2.5} > 35\ \mu g\ m^{-3}$) for a larger fraction of the population than a similar data set representing AOD from polar-orbiting satellites in 2020. Applying pre-existing estimates of the reduction in $PM_{2.5}$ exposure due to individual behavior modification in alerted populations, we estimate 54% more averted $PM_{2.5}$-attributable mortality, or 1,200 (800–1,500) deaths per year, using geostationary over polar-orbiting satellite data. These averted deaths are associated with an economic value of 13 (95% CI: 8.8–17) billion dollars ($2019) per year. There are many additional health benefits of reduced $PM_{2.5}$ exposure that are not quantified in this work, such as lost work days and inhaler medication refills, which impact a larger percentage of the population than the more severe health outcomes we quantify (U.S. EPA, 2022).

The magnitude and spatial distribution of alert days and subsequent benefits of identifying additional alert days will likely vary for different years. The total $PM_{2.5}$-attributable mortality we estimate using 2020 annual means (96,000 deaths) is within the range of previous estimates of $PM_{2.5}$-attributable mortality in the US (Ford et al., 2018; O'Dell et al., 2021; Tessum et al., 2019) and approximately double the 2019 GBD estimate of 50,000 $PM_{2.5}$-attributable deaths (GBD, 2019). Differences in these values predominantly come from differences in concentration response functions used and estimated $PM_{2.5}$ concentrations. We note 2020 was an exceptionally active wildfire year and had many $PM_{2.5}$ alert days in populated areas in the western US compared to other recent years. However, wildfire seasons worse than 2020 are projected to become at least twice as likely by 2050 in the US West under climate change (Abatzoglou et al., 2021; Xie et al., 2022). Thus, these results using 2020 data are likely more representative of benefits of geostationary satellites and nowcasting applications in the future compared to a recent less active fire year such as 2019. We expect our main conclusion that atmospheric

composition data from geostationary satellites is able to lead to additional exposure reduction by identifying more $PM_{2.5}$ alert days than polar-orbiting satellites to still hold for other, less active, wildfire years.

Our application of a health impact assessment to an alert/behavior modification pathway for $PM_{2.5}$ exposure reduction is novel and requires several assumptions when quantifying health benefits. First, the relative risk values and concentration response function we applied were developed using ambient outdoor $PM_{2.5}$ concentrations, not personal exposure. In addition, relative risk values may already incorporate some level of behavior modification that was taken by people in the cohorts studied to develop them. These assumptions have been made previously in estimating benefits of N95 masks for reducing wildfire smoke exposure (Kodros et al., 2021). We incorporate the uncertainty associated with the concentration response function in our health impact assessment, but there are additional sources of uncertainty from population estimates, baseline disease rates, $PM_{2.5}$ estimates, and the assumed exposure reduction in alerted populations. It is also currently uncertain how reductions in peak exposures to $PM_{2.5}$ translate to reduced health impacts of long-term exposure. However, this assumption is often made when assessing the contribution of wildfire smoke $PM_{2.5}$ to mortality from long-term $PM_{2.5}$ exposure (Ford et al., 2018; Neumann et al., 2021; O'Dell et al., 2021). Thus, despite our novel application of this pathway of exposure reduction in a health impact assessment, our applications of $PM_{2.5}$ concentration response functions are consistent with previous health impact assessments.

The relationship between $PM_{2.5}$ data sets and issuing air quality alerts is more complex in practice than we are able to represent in our methodology. First, we use a 24hr average concentration for flagging alert days and reduce exposure to the full 24hr average. In practice, the AirNow NowCast typically relies on weighted, rolling $PM_{2.5}$ concentration averages over the previous 12 hr (US EPA, 2021). However, we do not know in which hour people may modify their behavior to reduce exposure and a daily average exposure is required for the health impact assessment to align with the underlying epidemiology data. Second, our analysis assumes air quality alerts from national nowcasting based on these individual data sets are the only driver for behavior modification during pollution events. However, information from air quality forecasting (often based on numerical models along with satellite imagery), local air quality monitoring agencies, and personal awareness of poor air quality are additional drivers for action (Semenza et al., 2008; Wen et al., 2009). In practice, a combination of many of these tools is used to determine air quality alerts. Determining how to best incorporate satellite-based data products in the EPA's AirNow system is an ongoing effort (Bratburd et al., 2022). In this work, we do not prescribe how these tools may be used in practice, but rather investigate how these data sources may better inform air quality forecasters in their decision making.

The pathway from air quality alerts to reduced $PM_{2.5}$ exposure is also more complex than we are able to represent here. We assume the same percent reduction in $PM_{2.5}$ across all alerted populations yet in reality some communities or age groups may be more able or willing to modify their behavior than others (Burke et al., 2022; D'Antoni et al., 2017; Hano et al., 2020; Kolbe & Gilchrist, 2009; Mirabelli et al., 2018; Rappold et al., 2019). The exposure reduction values we use come from studies investigating responses to smoke events which estimate a likelihood of taking action (specifically remaining indoors) of ~60% (U.S. EPA, 2021). Studies of responses to all air pollution events and/or alerts (not smoke specific) often report smaller response rates (D'Antoni et al., 2017; McDermott et al., 2006; Wen et al., 2009). Given that 2020 was a very active fire year, and the likelihood of action on alert days is higher for smoke-impacted days, the magnitude of our results likely constitutes an upper bound on the averted premature deaths and associated economic benefits from nowcasting with geostationary over polar-orbiting satellite data. While these factors would impact the overall magnitude of the health benefits from expanded $PM_{2.5}$ nowcasting with geostationary satellite data, in this work we are more concerned with the relative difference in exposure reduction between the geostationary and polar-orbiting cases which are calculated under the same assumptions.

Our results have implications both for the application of current geostationary atmospheric composition data (like AOD from GOES) as well as planning for future geostationary satellite missions, such as NASA's TEMPO and NOAA's GeoXO mission. These future geostationary satellite missions have the potential to continue and expand upon the public health benefits of satellite-based atmospheric composition data applications. This work highlights one of the many advantages of using satellite data for air pollution monitoring. Atmospheric composition data from geostationary satellites will also provide valuable information for long-term $PM_{2.5}$ monitoring such as a greater capability to observe sub-daily patterns in emissions sources which could potentially be applied to design more effective and health-beneficial approaches for reducing ambient $PM_{2.5}$ concentrations. Pathways to

quantify the health benefits of these additional applications of geostationary satellite data should be explored in future works. The work presented here shows satellite data, in particular geostationary satellite data, can be used to inform personal adaptation to short-term $PM_{2.5}$ pollution events for a greater number of people, leading to a reduction in the negative health impacts of poor air quality. Future cost-benefit analyses of satellite missions should incorporate these and other health and economic benefits of monitoring and reducing exposure to air pollution. It will be important to ensure these benefits are realized by working with decision makers and local actors to incorporate these data sets into national and local air quality decision-making.

Disclaimer

The views expressed in this article are those of the authors and do not necessarily represent the views or policies of the U.S. Environmental Protection Agency. Further, the contents of this article are the authors and do not necessarily reflect any position of the Government or the National Oceanic and Atmospheric Administration.

Conflict of Interest

KO reports honoraria from NOAA during the conduct of the study. DG reports grants from NOAA during the conduct of the study. GHK reports personal fees from California Air Resources Board, personal fees from Department of Justice, personal fees from New York State Attorney General, and personal fees from Environmental Defense Fund outside the submitted work. BH, HZ, SCA, SK, and ZW have no conflicts of interest to declare relevant to the present study.

Data Availability Statement

The computer code used for the analysis presented in this manuscript are publicly available on GitHub (O'Dell, 2023). Gridded population data (NASA SEDAC, 2018), ZCTA-level population data (Manson et al., 2022), county-level baseline disease rates (CDC, 2021), and the AirNow data (US EPA, 2023) are publicly available. Satellite-based data sets are available for download (O'Dell et al., 2023).

Acknowledgments
We gratefully acknowledge the computational resouces provided by George Washington University's High Performance Computing Cluster operated by the Research Technology Services team (MacLachlan et al., 2020), much of the computational analysis here would have been exceedingly time consuming without them. We are grateful to those who support and maintain the public data sources used in this work described in the Data Availability Statement Finally, we express our gratitude to Gregory Frost for many helpful discussions about this work throughout the project. K.O., D.G., G.H.K., and S.A. acknowledge research support for this work from NOAA (Contract 1305M322PNRMT0426 and Grant NA21OAR4310250).

References

Abatzoglou, J. T., Battisti, D. S., Williams, A. P., Hansen, W. D., Harvey, B. J., & Kolden, C. A. (2021). Projected increases in western US forest fire despite growing fuel constraints. *Communications Earth & Environment*, *2*(1), 227. Article 1. https://doi.org/10.1038/s43247-021-00299-0

Abatzoglou, J. T., & Williams, A. P. (2016). Impact of anthropogenic climate change on wildfire across western US forests. *Proceedings of the National Academy of Sciences of the United States of America*, *113*(42), 11770–11775. https://doi.org/10.1073/pnas.1607171113

AHRQ. (2006). HCUP Databases. Healthcare cost and utilization project (HCUP) [Dataset]. Retrieved from www.hcup-us.ahrq.gov/databases.jsp

Anenberg, S. C., Bindl, M., Brauer, M., Castillo, J. J., Cavalieri, S., Duncan, B. N., et al. (2020). Using satellites to track indicators of global air pollution and climate change impacts: Lessons learned from a NASA-supported science-stakeholder collaborative. *GeoHealth*, *4*(7), e2020GH000270. https://doi.org/10.1029/2020GH000270

Anenberg, S. C., Henze, D. K., Tinney, V., Kinney, P. L., Raich, W., Fann, N., et al. (2018). Estimates of the Global Burden of Ambient $PM_{2.5}$, Ozone, and NO_2 on asthma incidence and emergency room visits. *Environmental Health Perspectives*, *126*(10), 107004. https://doi.org/10.1289/EHP3766

Anenberg, S. C., Horowitz, H. L., Tong, D. Q., & West, J. J. (2010). An estimate of the global burden of anthropogenic ozone and fine particulate matter on premature human mortality using atmospheric modeling. *Environmental Health Perspectives*, *118*(9), 1189–1195. https://doi.org/10.1289/ehp.0901220

Anenberg, S. C., West, J. J., Yu, H., Chin, M., Schulz, M., Bergmann, D., et al. (2014). Impacts of intercontinental transport of anthropogenic fine particulate matter on human mortality. *Air Quality, Atmosphere & Health*, *7*(3), 369–379. https://doi.org/10.1007/s11869-014-0248-9

Bratburd, J., Gupta, P., Kondragunta, S., Zhang, H., Henderson, B. H., Dickerson, P., et al. (2022). Incorporating satellite data updates into AirNow. *Em PLUS*. Retrieved from https://haqast.org/wp-content/uploads/sites/91/2022/09/emplusq322_bratburd-final.pdf

Burke, M., Heft-Neal, S., Li, J., Driscoll, A., Baylis, P., Stigler, M., et al. (2022). Exposures and behavioural responses to wildfire smoke. *Nature Human Behaviour*, *6*(10), 1351–1361. Article 10. https://doi.org/10.1038/s41562-022-01396-6

Castillo, M. D., Kinney, P. L., Southerland, V., Arno, C. A., Crawford, K., van Donkelaar, A., et al. (2021). Estimating intra-urban inequities in $PM_{2.5}$-attributable health impacts: A case study for Washington, DC. *GeoHealth*, *5*(11), e2021GH000431. https://doi.org/10.1029/2021GH000431

CDC. (2021). Centers for disease control and prevention, national center for health statistics. National vital statistics. Mortality 1999-2020 on CDC WONDER online database [Dataset]. CDC. Retrieved from http://wonder.cdc.gov/ucd-icd10.html

Chen, H., Li, Q., Kaufman, J. S., Wang, J., Copes, R., Su, Y., & Benmarhnia, T. (2018). Effect of air quality alerts on human health: A regression discontinuity analysis in Toronto, Canada. *The Lancet Planetary Health*, *2*(1), e19–e26. https://doi.org/10.1016/S2542-5196(17)30185-7

Childs, M. L., Li, J., Wen, J., Heft-Neal, S., Driscoll, A., Wang, S., et al. (2022). Daily local-level estimates of ambient wildfire smoke $PM_{2.5}$ for the contiguous US. *Environmental Science & Technology*, *56*(19), 13607–13621. https://doi.org/10.1021/acs.est.2c02934

Clean Air Partners. (2018). Clean air partners 2018 public awareness survey. Retrieved from https://www.mwcog.org/assets/1/25/Clean_Air_Partners_2018_Regional_Survey_Final_Report_050819_reducedsize.pdf

Dai, L., Zanobetti, A., Koutrakis, P., & Schwartz, J. D. (2014). Associations of fine particulate matter species with mortality in the United States: A multicity time-series analysis. *Environmental Health Perspectives*, *122*(8), 837–842. https://doi.org/10.1289/ehp.1307568

D'Antoni, D., Smith, L., Auyeung, V., & Weinman, J. (2017). Psychosocial and demographic predictors of adherence and non-adherence to health advice accompanying air quality warning systems: A systematic review. *Environmental Health*, *16*(1), 100. https://doi.org/10.1186/s12940-017-0307-4

David, L. M., Ravishankara, A. R., Brey, S. J., Fischer, E. V., Volckens, J., & Kreidenweis, S. (2021). Could the exception become the rule? "Uncontrollable" air pollution events in the U.S. due to wildland fires. *Environmental Research Letters*. https://doi.org/10.1088/1748-9326/abe1f3

Di, Q., Amini, H., Shi, L., Kloog, I., Silvern, R., Kelly, J., et al. (2019). An ensemble-based model of $PM_{2.5}$ concentration across the contiguous United States with high spatiotemporal resolution. *Environment International*, *130*, 104909. https://doi.org/10.1016/j.envint.2019.104909

Diao, M., Holloway, T., Choi, S., O'Neill, S. M., Al-Hamdan, M. Z., Van Donkelaar, A., et al. (2019). Methods, availability, and applications of PM2.5 exposure estimates derived from ground measurements, satellite, and atmospheric models. *Journal of the Air & Waste Management Association*, *69*(12), 1391–1414. https://doi.org/10.1080/10962247.2019.1668498

Ford, B., Martin, M. V., Zelasky, S. E., Fischer, E. V., Anenberg, S. C., Heald, C. L., & Pierce, J. R. (2018). Future fire impacts on smoke concentrations, visibility, and health in the contiguous United States. *GeoHealth*, *2*(8), 229–247. https://doi.org/10.1029/2018GH000144

GBD. (2019). *Global burden of disease collaborative network. Global burden of disease study 2019 (GBD 2019) results*. Institute for Health Metrics and Evaluation (IHME). Retrieved from http://ghdx.healthdata.org/gbd-results-tool

Geng, G., Murray, N. L., Tong, D., Fu, J. S., Hu, X., Lee, P., et al. (2018). Satellite-based daily $PM_{2.5}$ estimates during fire seasons in Colorado. *Journal of Geophysical Research: Atmospheres*, *123*(15), 8159–8171. https://doi.org/10.1029/2018JD028573

Hammer, M. S., van Donkelaar, A., Li, C., Lyapustin, A., Sayer, A. M., Hsu, N. C., et al. (2020). Global estimates and long-term trends of fine particulate matter concentrations (1998–2018). *Environmental Science & Technology*, *54*(13), 7879–7890. https://doi.org/10.1021/acs.est.0c01764

Hano, M. C., Prince, S. E., Wei, L., Hubbell, B. J., & Rappold, A. G. (2020). Knowing your audience: A typology of smoke sense participants to inform wildfire smoke health risk communication. *Frontiers in Public Health*, *8*. https://doi.org/10.3389/fpubh.2020.00143

Healthcare Use Data | CDC. (2023). Healthcare use data | CDC [Dataset]. Retrieved from https://www.cdc.gov/asthma/healthcare-use/2018/table_a.html

Holloway, T., Miller, D., Anenberg, S., Diao, M., Duncan, B., Fiore, A. M., et al. (2021). Satellite monitoring for air quality and health. *Annual Review of Biomedical Data Science*, *4*(1), 417–447. https://doi.org/10.1146/annurev-biodatasci-110920-093120

Huff, A. K., & Kondragunta, S. (2017). Meteorologists track wildfires using satellite smoke images. *Eos*. https://doi.org/10.1029/2017EO070275

Huff, A. K., Kondragunta, S., Zhang, H., Laszlo, I., Zhou, M., Caicedo, V., et al. (2021). Tracking smoke from a prescribed fire and its impacts on local air quality using temporally resolved GOES-16 ABI aerosol optical depth (AOD). *Journal of Atmospheric and Oceanic Technology*, *38*(5), 963–976. https://doi.org/10.1175/JTECH-D-20-0162.1

Jaffe, D., Hafner, W., Chand, D., Westerling, A., & Spracklen, D. (2008). Interannual variations in $PM_{2.5}$ due to wildfires in the Western United States. *Environmental Science & Technology*, *42*(8), 2812–2818. https://doi.org/10.1021/es702755v

Kerr, G. H., Martin, R. V., Van Donkelaar, A., Brauer, M., Bukart, K., Wozniak, S., et al. (2022). Increasing disparities in air pollution health burdens in the United States [Dataset]. Environmental Sciences. [Preprint]. https://doi.org/10.1002/essoar.10512159.1

Kodros, J. K., O'Dell, K., Samet, J. M., L'Orange, C., Pierce, J. R., & Volckens, J. (2021). Quantifying the health benefits of face masks and respirators to mitigate exposure to severe air pollution. *GeoHealth*, *5*(9), e2021GH000482. https://doi.org/10.1029/2021GH000482

Kolbe, A., & Gilchrist, K. L. (2009). An extreme bushfire smoke pollution event: Health impacts and public health challenges. *NSW Public Health Bulletin*, *20*(2), 19–23. https://doi.org/10.1071/NB08061

Kondragunta, S., Laszlo, I., Zhang, H., Ciren, P., & Huff, A. (2020). Chapter 17—Air quality applications of ABI aerosol products from the GOES-R series. In S. J. Goodman, T. J. Schmit, J. Daniels, & R. J. Redmon (Eds.), *The GOES-R series* (pp. 203–217). Elsevier. https://doi.org/10.1016/B978-0-12-814327-8.00017-2

Liu, H., Remer, L. A., Huang, J., Huang, H.-C., Kondragunta, S., Laszlo, I., et al. (2014). Preliminary evaluation of S-NPP VIIRS aerosol optical thickness. *Journal of Geophysical Research: Atmospheres*, *119*(7), 3942–3962. https://doi.org/10.1002/2013JD020360

Liu, J., Clark, L. P., Bechle, M. J., Hajat, A., Kim, S.-Y., Robinson, A. L., et al. (2021). Disparities in air pollution exposure in the United States by race/ethnicity and income, 1990–2010. *Environmental Health Perspectives*, *129*(12), 127005. https://doi.org/10.1289/EHP8584

MacLachlan, G., Hurlburt, J., Suarez, M., Wong, K. L., Burke, W., Lewis, T., et al. (2020). Building a shared resource HPC center across university schools and institutes: A case study. (arXiv:2003.13629). arXiv. https://doi.org/10.48550/arXiv.2003.13629

Malm, W. C., Schichtel, B. A., Hand, J. L., & Collett, J. L. (2017). Concurrent temporal and spatial trends in sulfate and organic mass concentrations measured in the IMPROVE monitoring program. *Journal of Geophysical Research: Atmospheres*, *122*(19), 2017JD026865. https://doi.org/10.1002/2017JD026865

Manson, S., Schroeder, J., Van Riper, D., Kugler, T., & Ruggles, S. (2022). IPUMS national historical geographic information system (17.0) [2020 American community survey: 5-Year data [2016-2020, block groups & larger areas]] [Dataset]. IPUMS. https://doi.org/10.18128/D050.V17.0

McClure, C. D., & Jaffe, D. A. (2018). US particulate matter air quality improves except in wildfire-prone areas. *Proceedings of the National Academy of Sciences of the United States of America*, *115*(31), 7901–7906. https://doi.org/10.1073/pnas.1804353115

McDermott, M., Srivastava, R., & Croskell, S. (2006). Awareness of and compliance with air pollution advisories: A comparison of parents of asthmatics with other parents. *Journal of Asthma*, *43*(3), 235–239. https://doi.org/10.1080/02770900600567114

Mirabelli, M. C., Boehmer, T. K., Damon, S. A., Sircar, K. D., Wall, H. K., Yip, F. Y., et al. (2018). Air quality awareness among U.S. adults with respiratory and heart disease. *American Journal of Preventive Medicine*, *54*(5), 679–687. https://doi.org/10.1016/j.amepre.2018.01.037

NASA SEDAC. (2018). Documentation for the gridded population of the world, version 4 (GPWv4), revision 11 data sets [Dataset]. NASA Socioeconomic Data and Applications Center (SEDAC). https://doi.org/10.1007/s11869-010-0125-0

Neumann, J. E., Amend, M., Anenberg, S. C., Kinney, P. L., Sarofim, M., Martinich, J., et al. (2021). Estimating $PM_{2.5}$-related premature mortality and morbidity associated with future wildfire emissions in the western U.S. *Environmental Research Letters*, *16*(3), 035019. https://doi.org/10.1088/1748-9326/abe82b

O'Dell, K. (2023). Release a0 · kaodell/GeoXO [Computer Software]. Zenodo. https://doi.org/10.5281/zenodo.8384660

O'Dell, K., Bilsback, K., Ford, B., Martenies, S. E., Magzamen, S., Fischer, E. V., & Pierce, J. R. (2021). Estimated mortality and morbidity attributable to smoke plumes in the United States: Not just a western US Problem. *GeoHealth*, *5*(9), e2021GH000457. https://doi.org/10.1029/2021GH000457

O'Dell, K., Ford, B., Fischer, E. V., & Pierce, J. R. (2019). Contribution of wildland-fire smoke to US $PM_{2.5}$ and its influence on recent trends. *Environmental Science & Technology*, *53*(4), 1797–1804. https://doi.org/10.1021/acs.est.8b05430

O'Dell, K., Kondragunta, S., Zhang, H., Goldberg, D. L., Kerr, G. H., Wei, Z., et al. (2023). Dataset for "Public health benefits from improved identification of severe air pollution events with geostationary satellite data" [Dataset]. Zenodo. https://doi.org/10.5281/zenodo.10058357

O'Neill, S., & Raffuse, S. (2021). Advances in satellite data for wildfire smoke forecasting. *Eos*, *102*. https://doi.org/10.1029/2021EO155076

Orellano, P., Quaranta, N., Reynoso, J., Balbi, B., & Vasquez, J. (2017). Effect of outdoor air pollution on asthma exacerbations in children and adults: Systematic review and multilevel meta-analysis. *PLoS One*, *12*(3), e0174050. https://doi.org/10.1371/journal.pone.0174050

Rappold, A. G., Hano, M. C., Prince, S., Wei, L., Huang, S. M., Baghdikian, C., et al. (2019). Smoke sense initiative leverages citizen science to address the growing wildfire-related public health problem. *GeoHealth*, *3*(12), 443–457. https://doi.org/10.1029/2019GH000199

Rappold, A. G., Reyes, J., Pouliot, G., Cascio, W. E., & Diaz-Sanchez, D. (2017). Community vulnerability to health impacts of wildland fire smoke exposure. *Environmental Science & Technology*, *51*(12), 6674–6682. https://doi.org/10.1021/acs.est.6b06200

Rappold, A. G., Stone, S. L., Cascio, W. E., Neas, L. M., Kilaru, V. J., Carraway, M. S., et al. (2011). Peat bog wildfire smoke exposure in rural North Carolina is associated with cardiopulmonary emergency department visits assessed through syndromic surveillance. *Environmental Health Perspectives*, *119*(10), 1415–1420. https://doi.org/10.1289/ehp.1003206

Ridley, D. A., Heald, C. L., Ridley, K. J., & Kroll, J. H. (2018). Causes and consequences of decreasing atmospheric organic aerosol in the United States. *Proceedings of the National Academy of Sciences of the United States of America*, *115*(2), 290–295. https://doi.org/10.1073/pnas.1700387115

Schmit, T. J., Gunshor, M. M., Menzel, W. P., Gurka, J. J., Li, J., & Bachmeier, A. S. (2005). Introducing the next-generation advanced baseline imager on GOES-R. *Bulletin of the American Meteorological Society*, *86*(8), 1079–1096. https://doi.org/10.1175/BAMS-86-8-1079

Schmit, T. J., Lindstrom, S. S., Gerth, J. L., & Gunshor, M. M. (2018). Applications of the 16 spectral bands on the advanced baseline imager (ABI). *Journal of Operational Meteorology*, *6*(4), 33–46. https://doi.org/10.15191/nwajom.2018.0604

Semenza, J. C., Wilson, D. J., Parra, J., Bontempo, B. D., Hart, M., Sailor, D. J., & George, L. A. (2008). Public perception and behavior change in relationship to hot weather and air pollution. *Environmental Research*, *107*(3), 401–411. https://doi.org/10.1016/j.envres.2008.03.005

Spracklen, D. V., Logan, J. A., Mickley, L. J., Park, R. C., Yevich, R., Westerling, A. L., & Jaffe, D. A. (2007). Wildfires drive interannual variability of organic carbon aerosol in the western U.S. in summer. *Geophysical Research Letters*, *34*(16), L16816. https://doi.org/10.1029/2007GL030037

Tessum, C. W., Apte, J. S., Goodkind, A. L., Muller, N. Z., Mullins, K. A., Paolella, D. A., et al. (2019). Inequity in consumption of goods and services adds to racial–ethnic disparities in air pollution exposure. *Proceedings of the National Academy of Sciences of the United States of America*, *116*(13), 6001–6006. https://doi.org/10.1073/pnas.1818859116

Turner, M. C., Jerrett, M., Pope, C. A., Krewski, D., Gapstur, S. M., Diver, W. R., et al. (2016). Long-term ozone exposure and mortality in a large prospective study. *American Journal of Respiratory and Critical Care Medicine*, *193*(10), 1134–1142. https://doi.org/10.1164/rccm.201508-1633OC

U.S. DOT. (2023). Departmental guidance on valuation of a statistical life in economic analysis. Webpage. Retrieved from https://www.transportation.gov/office-policy/transportation-policy/revised-departmental-guidance-on-valuation-of-a-statistical-life-in-economic-analysis

U.S. EPA. (2010). Guidelines for preparing economic analyses (other policies and guidance 240-R-10-001). Retrieved from https://www.epa.gov/environmental-economics/guidelines-preparing-economic-analyses

U.S. EPA. (2021). Comparative assessment of the impacts of prescribed fire versus wildfire (CAIF): A case study in the western U.S. (EPA/600/R-21/197).

US EPA. (2021). AirNow—How is the NowCast algorithm used to report current air quality? AirNow. Retrieved from https://usepa.servicenow-services.com/airnow?id=kb_article_view&sysparm_article=KB0011856

U.S. EPA. (2022). *Supplement to the 2019 integrated science assessment for particulate matter*. U.S. Environmental Protection Agency. EPA/635/R-22/028.

US EPA. (2023). Air quality system data mart [Internet database]. Retrieved from https://www.epa.gov/outdoor-air-quality-data

van Donkelaar, A., Hammer, M. S., Bindle, L., Brauer, M., Brook, J. R., Garay, M. J., et al. (2021). Monthly global estimates of fine particulate matter and their uncertainty. *Environmental Science & Technology*, *55*(22), 15287–15300. https://doi.org/10.1021/acs.est.1c05309

Vu, B. N., Bi, J., Wang, W., Huff, A., Kondragunta, S., & Liu, Y. (2022). Application of geostationary satellite and high-resolution meteorology data in estimating hourly $PM_{2.5}$ levels during the camp fire episode in California. *Remote Sensing of Environment*, *271*, 112890. https://doi.org/10.1016/j.rse.2022.112890

Wang, Y., Hu, X., Chang, H. H., Waller, L. A., Belle, J. H., & Liu, Y. (2018). A Bayesian Downscaler model to estimate daily $PM_{2.5}$ levels in the conterminous US. *International Journal of Environmental Research and Public Health*, *15*(9), Article 9. https://doi.org/10.3390/ijerph15091999

Wen, X.-J., Balluz, L., & Mokdad, A. (2009). Association between media alerts of air quality index and change of outdoor activity among adult asthma in six states, BRFSS, 2005. *Journal of Community Health*, *34*(1), 40–46. https://doi.org/10.1007/s10900-008-9126-4

Westerling, A. L. (2016). Increasing western US forest wildfire activity: Sensitivity to changes in the timing of spring. *Philosophical Transactions of the Royal Society B*, *371*(1696), 20150178. https://doi.org/10.1098/rstb.2015.0178

Xie, Y., Lin, M., Decharme, B., Delire, C., Horowitz, L. W., Lawrence, D. M., et al. (2022). Tripling of western US particulate pollution from wildfires in a warming climate. *Proceedings of the National Academy of Sciences of the United States of America*, *119*(14), e2111372119. https://doi.org/10.1073/pnas.2111372119

Zhang, H., & Kondragunta, S. (2021). Daily and hourly surface $PM_{2.5}$ estimation from satellite AOD. *Earth and Space Science*, *8*(3), e2020EA001599. https://doi.org/10.1029/2020EA001599

Zhang, H., Kondragunta, S., Laszlo, I., Liu, H., Remer, L. A., Huang, J., et al. (2016). An enhanced VIIRS aerosol optical thickness (AOT) retrieval algorithm over land using a global surface reflectance ratio database. *Journal of Geophysical Research: Atmospheres*, *121*(18), 10717–10738. https://doi.org/10.1002/2016JD024859

Zhang, H., Kondragunta, S., Laszlo, I., & Zhou, M. (2020). Improving GOES advanced baseline imager (ABI) aerosol optical depth (AOD) retrievals using an empirical bias correction algorithm. *Atmospheric Measurement Techniques*, *13*(11), 5955–5975. https://doi.org/10.5194/amt-13-5955-2020

Zhang, H., Wei, Z., Henderson, B. H., Anenberg, S. C., O'Dell, K., & Kondragunta, S. (2022). Nowcasting applications of geostationary satellite hourly surface $PM_{2.5}$ Data. *Weather and Forecasting*, *37*(12), 2313–2329. https://doi.org/10.1175/WAF-D-22-0114.1

Zoogman, P., Liu, X., Suleiman, R. M., Pennington, W. F., Flittner, D. E., Al-Saadi, J. A., et al. (2017). Tropospheric emissions: Monitoring of pollution (TEMPO). *Journal of Quantitative Spectroscopy and Radiative Transfer*, *186*, 17–39. https://doi.org/10.1016/j.jqsrt.2016.05.008